# CATALYTIC REACTOR STUDIES

_____

**FINAL REPORT**
**SEPTEMBER 2001**

KLK317
N01-17

_____

Prepared for

**OFFICE OF UNIVERSITY RESEARCH AND EDUCATION**

**U.S. DEPARTMENT OF TRANSPORTATION**

Prepared by

**NIATT**

**NATIONAL INSTITUTE FOR ADVANCED TRANSPORTATION TECHNOLOGY**

**UNIVERSITY OF IDAHO**

Judi Steciak, PhD, P.E.

Steven Beyerlein, PhD

Heather Jones

Mike Klein

Steve Kramer

Xiangyang Wang

# CATALYTIC REACTOR STUDIES

Judi Steciak, PhD, P.E.

Steven Beyerlein, PhD

Heather Jones

Mike Klein

Steve Kramer

Xiangyang Wang

**TABLE OF CONTENTS**

# EXECUTIVE SUMMARY

Progress was made in *hardware development, equilibrium calculations* and with *understanding combustion kinetics*.

The design and construction of a plug flow, pressurized reactor is well underway. A literature search identified design and safety concerns for similar reactors. The vaporizer section was constructed. A prototype mixing valve was machined.

The thermodynamic equilibrium calculations are finished for ethanol-water volume fractions ranging from 0 to 0.5; equivalence ratios ranging between 0.4 and 1.6 (fuel lean to fuel rich); and pressures ranging from 1 to 16 atmospheres. The calculations show the influence of the water-gas shift reaction on the increased oxidation of carbon monoxide with increased fuel water content. The impact of water on NO formation can be roughly explained by the sensitivity of the thermal NO mechanism to decreasing combustion temperature with increasing water-fuel content.

Good progress has been made understanding the gas phase and surface reactions of ethanol. Three major pathways are present for gas-phase ethanol combustion based on the three radicals formed when an H atom is stripped from one of the three backbone atoms in the molecule ($C_1$, $C_2$ or O). Acetaldehyde, ethene and formaldehyde are stable intermediate products depending on the pathway, with the acetaldehyde path dominating.

In the presence of the catalyst, hydrogen atoms are stripped off the ethanol molecule because of the proximity effect of the platinum (Pt) surface. Pt surface reactions produce stable products, radicals, and heat. The chemical species that can desorb include OH radicals. Products, radicals and heat diffuse from the surface to unreacted gas-phase ethanol where ignition occurs.

HCT is a finite-difference code that calculates one-dimensional time-dependent problems involving gas hydrodynamics, transport, and detailed chemical kinetics. A one-dimensional catalytic surface reaction model is under development for addition to the code.

## DESCRIPTION OF PROBLEM

Introducing catalytic surfaces in combustion systems supplies an additional control parameter, namely the surface reaction rate. Diffusion of energy and intermediate species released from exothermic surface reaction can dramatically accelerate gas phase reaction. While there have been many studies of catalytic oxidation of hydrocarbons, the majority examine dry gaseous fuels, and only a few studies have examined catalytic oxidation in the presence of water vapor. The objective of this multi-year project is to produce a model that accurately predicts heterogeneous and homogeneous ignition over a range of fuel types, fuel-water mixtures, and initial thermal conditions. Data for this model will be generated from flow reactor studies and spectroscopic characterization of catalytic surfaces taken from different operating environments.

# APPROACH AND METHODOLOGY

To understand the ethanol-water gas phase and surface mechanisms, we are investigating both experimental and modeling issues. Our experimental approach includes the design, construction and testing of a plug flow reactor that can be pressurized to typical pre-ignition engine conditions. Our modeling approach includes thermodynamic calculations at different ethanol-water volume factions, equivalence ratios, and pressures. Detailed chemical kinetic modeling of gas-phase and surface reactions, coupled with experimental results, should permit us to develop a simplified model that accurately predicts ignition. Our approach is summarized in the following outline.

1. Pressurizable plug-flow reactor
   a. Design concept
   b. Safety
   c. Fabrication
2. Model major chemical events expected in reactor
   a. Thermodynamic equilibrium
   b. Chemical kinetics
      i. Gas phase
      ii. Surface reactions

# FINDINGS; CONCLUSIONS; RECOMMENDATIONS

Progress was made in *hardware development, equilibrium calculations* and with *understanding combustion kinetics*.

## I. Hardware

The schematic in Fig. 1.1 illustrates the vaporizing, mixing, flow, and combustion sections of the pressurizable reactor. Initially, a small syringe pump will inject fuel into the vaporizer section. Fuel is injected into a porous wick surrounding the 750-watt coil heater where capillary action will bring the fuel to the wick surface. Nitrogen transports evaporated fuel into the mixing section where oxygen is introduced to achieve the desired equivalence ratio.
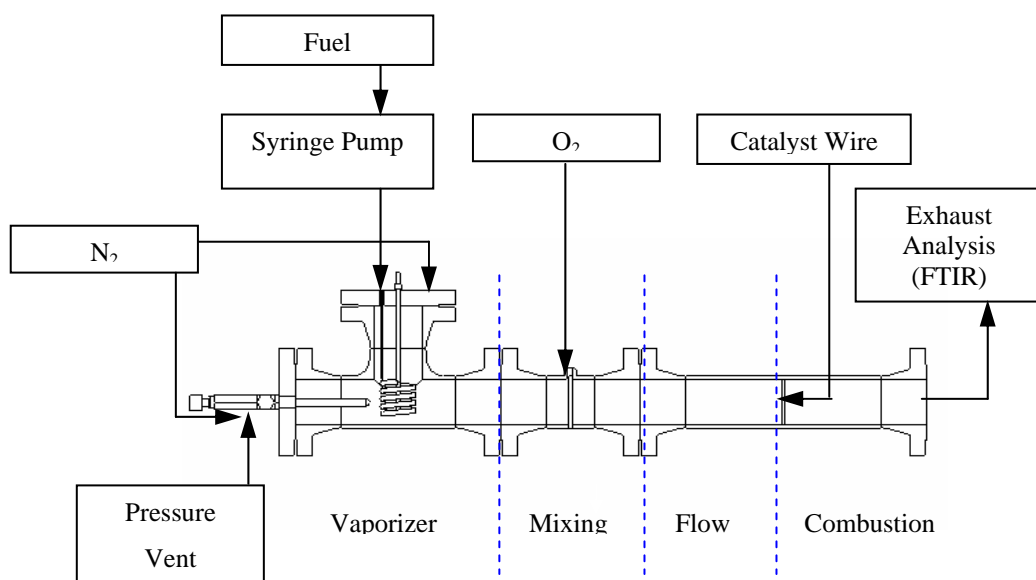
**Figure 1.1 Schematic of the flow reactor**

Separation of fuel and oxygen injection reduces the likelihood of spurious ignition caused by an electrical fault in the heater. The design of the mixing section minimizes the mixing time and ensures complete mixing. A turbulence grid injection system is used as a mixing nozzle.

In the mixing nozzle, the nitrogen-fuel mixture tapers into a tube (the diffuser, Fig. 1.2) and is vented outwards through six smaller holes, similar to a design developed at Drexel University [Koert, 1990]. The oxygen will enter through the middle ring where it fills a large cavity and enters the mixing area via 18 small holes. A sleeve creates the outside wall of the cavity, forming a plenum, where oxygen enters.
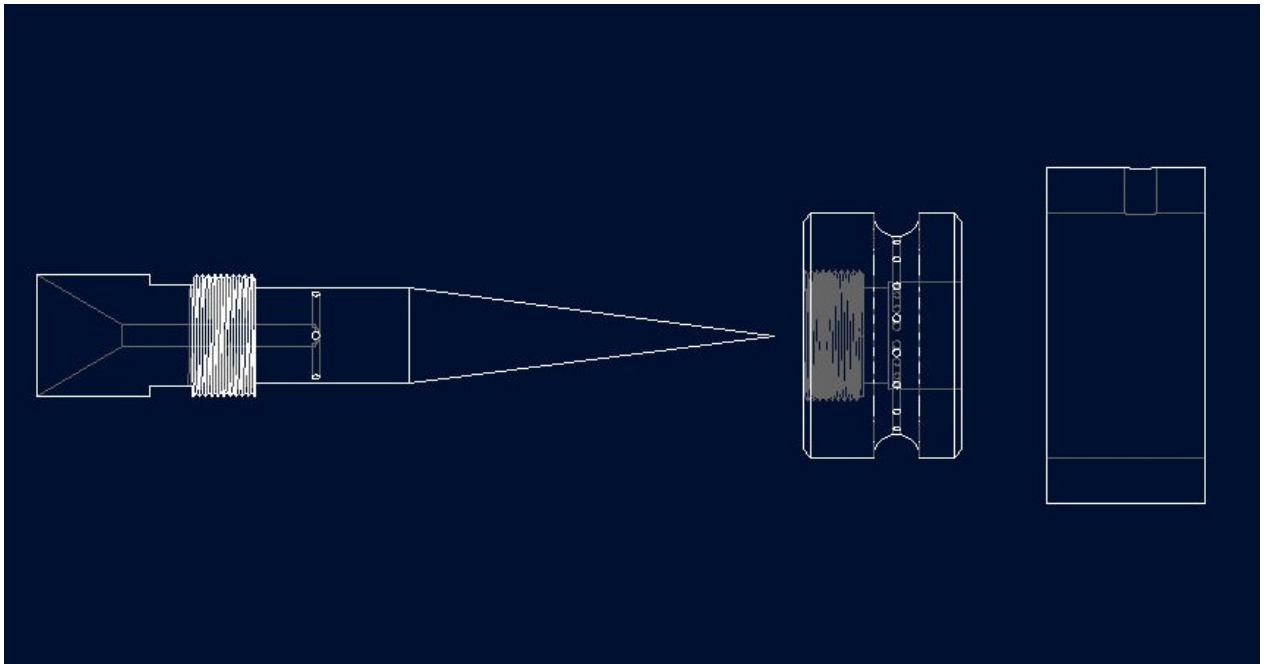


**Figure 1.2  The three sections of the mixing nozzle (L to R): diffuser, middle, and sleeve.**

A prototype mixing nozzle was machined from polymethyl methacrylate (Plexiglas®) and tested for fit with the evaporator section (Fig. 1.3). The gas-gas mixing nozzle design aims to preserve a step-change when the concentration of one gas stream—the fuel-nitrogen stream—is suddenly changed. Flow visualization of the mixing nozzle is required to determine how well the gases are mixing, and if the step-change is maintained. Useful tests will include flow visualization of one and then multiple orifices to see swirling effects at different distances from a clear flat plate. A smoke generator will be used to see the flow straight on and perpendicular to the flow. The smoke generator could also be used to show the flow in the existing mixing section.

Also, quantitative data taken will be obtained by introducing known flows of an inert gas (nitrogen) and a sensible gas ($CO_2$ diluted in nitrogen at a known concentration) into the mixing section. The test will start by having two streams of $N_2$ entering the mixing nozzle. A two-way valve will suddenly switch one stream from $N_2$ to a $CO_2$-$N_2$ blend; the step change in $CO_2$ concentration should be maintained and be able to be sensed downstream.
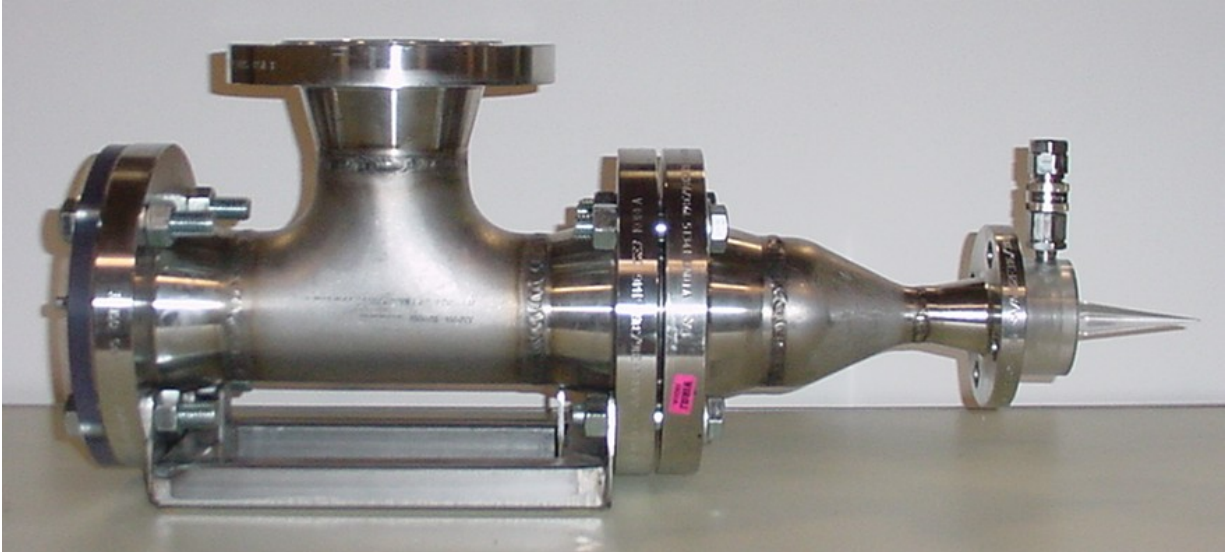


**Figure 1.3 Prototype mixing nozzle mounted downstream of the evaporator.**

The flow section ensures plug flow—a uniform cross section of temperature, velocity, and concentration. The combustion section of the reactor will contain catalysts in different arrangement as needed for experimentation. For example, some tests will use a platinum catalyst wire for igniting the fuel-air mixture. Instrumentation and calculations related to the wire will be used to determine the transition temperature from kinetic to diffusion control of the ignition process, based on the experimental method of Schwartz, et al. [1971]. Other tests will use a catalyst bed (for example, a bed of beads coated with platinum, or a honeycomb ceramic monolith coated with platinum) to obtain complete conversion of the fuel-air mixtures to combustion products.

A literature search for flow reactor systems provided information about standard designs features of reactors for combustion studies. Table 1.1 summarizes the nominal operating

ranges for the reactor based on the work of Koert [1990], Hoffman, et al. [1991], Dryer [1972], Karim, et al. [1994], Vermeersch, et al. [1991], Mao and Barat [1996], Marr, et al. [1992], and Dagaut, et al. [1986].

The literature summary shows that the FTIR gas analysis system that will be used in the reactor experiments has been used successfully for combustion product analysis of this kind. The quartz liners many of the researchers added to the system were intended to minimize reactions between the fuel-air mixture and the reactor walls. Experimental techniques will be used to remove the issue of wall reactions for the University of Idaho flow reactor. Cooled sampling probes are necessary for examination of species at intermediate points in the combustion process. Probes may be incorporated in the design at a later date, as experimentation requires. The range of the spatial and temporal values shown in Table 1.1 will be a guide for the design of the later sections of the reactor.

**Table 1.1   Summary of design parameters from reactor literature**

| Operating Parameter | | Range |
|---|---|---|
| Diameter | cm | 2.2  – 10.0 |
| Reactor Length | cm | 30.0 - 80.0 |
| Mixing Length | cm | 20.0 |
| Maximum Pressure | atm | 1 – 28 |
| Maximum Temperature | K | 1000 – 1700 |
| Reynolds Number | | Turbulent: Koert, Dryer, Hoffman<br>Laminar: Karim |
| Residence Time | ms | 2 – 250 |
| Mixing Time | ms | 1 – 10 |
| Velocity | cm/s | 50 – 700 |
| Cooled Sampling Probe | Common | Used by Koert, Dryer, Hoffman, Dagaut, Mao, Marr |
| Quartz Liner | Common | Used by Koert, Dryer, Dagaut, Vermeersch |
| Analysis Systems | | Gas Chromatography, Mass Spectroscopy,<br>FTIR, NDIR, NID |

Mitchell, et al. [1992] used the flow reactor described by Hoffman, et al. [1991] to compare the combustion of methanol in the reactor with the combustion of methanol in a diesel engine. Another key point from the literature involving safety, as discussed by Karim, et al. [1994], is that experiments conducted in a highly lean environment (equivalence ratio of 0.05) offer less potential for problems. Karim, et al. [1994], Dryer [1972], Hoffman, et al. [1991], Koert [1990], Mao and Barat [1996], and Vermeercsh, et al. [1991] also discuss surface reactions of catalysts and modeling the reactor system. The literature search provided specifications for the University of Idaho reactor design, operating parameters and introduced reactor hardware concepts used for previous research.

## II. Equilibrium Calculations and NO Formation

The composition of ethanol-water combustion products at equilibrium was calculated as a function of water content, equivalence ratio, and pressure. Modeling was done with

"EQLBRM," Gibbs free energy minimization software developed by the University of Washington [1988].

The graph shown in Figure 2.1 represents the equilibrium composition for a mixture of 30 percent water (by volume) at 1 atm and 298 K. The sixteen main equilibrium combustion products are shown as the equivalence ratio increases. The calculations provided general trends that may be quickly compared to the flow reactor results. The calculations also illustrate the impact of the water-gas shift reaction on the oxidation of CO with increasing water content in the fuel as shown in Fig.3. CO mole fraction decreases.

Most trends for change with water content are consistent through the pressure range. HCO, N, $N_2O$, $H_2O_2$, O, H, OH, $O_2$, $H_2$ species decrease with water addition. Morton [9] calculated a decrease of $NO_x$ species with increasing fuel water content and measured unusually low $NO_x$ partial pressures in ethanol-water fueled Diesel exhaust engine.
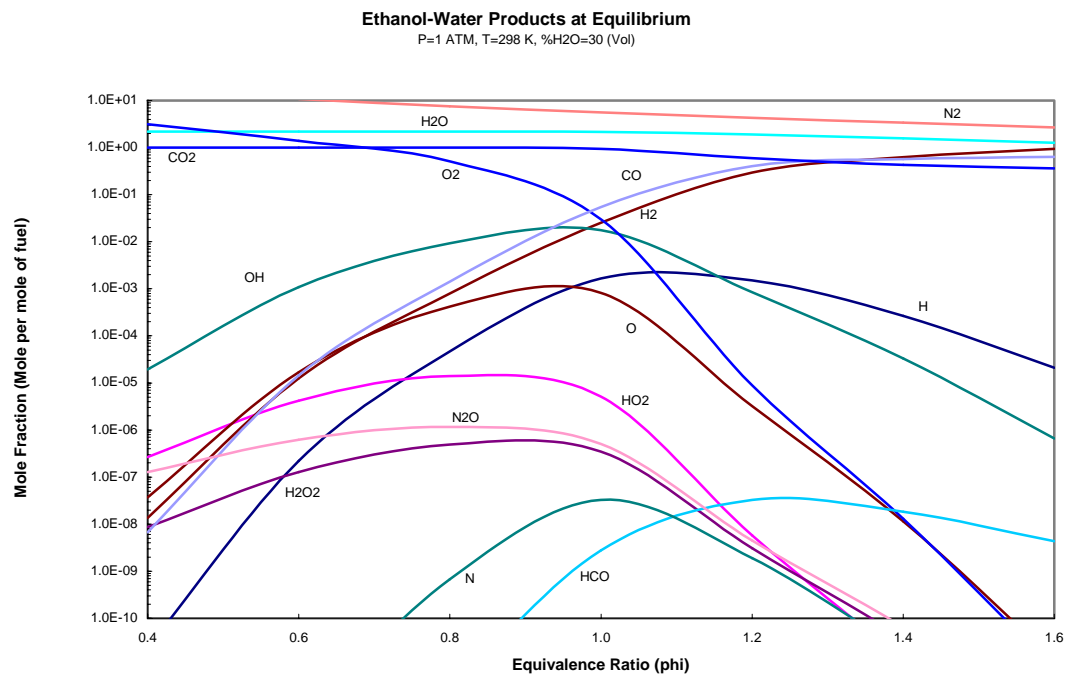


**Ethanol-Water Products at Equilibrium**
P=1 ATM, T=298 K, %H2O=30 (Vol)

**Figure 2.1 Equilibrium products vs. φ**

**Ethanol-Water Products at Equilibrium**
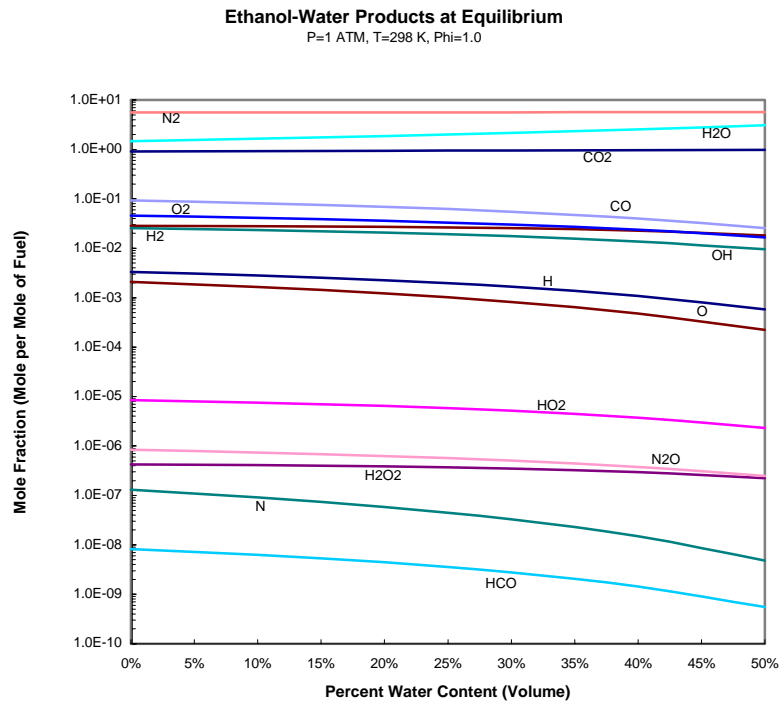P=1 ATM, T=298 K, Phi=1.0

**Figure2.2 Equilibrium Products vs. Fuel Water Content**

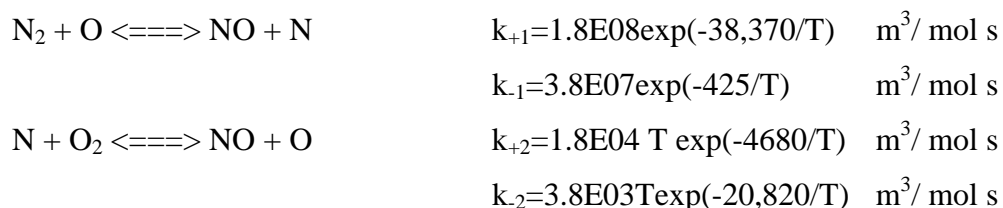## *Comparison of the Theoretical and Measured NO Production*

Equilibrium calculations do not account for the impact of chemical kinetics on species formation. The simplicity of the thermal or extended Zeldovich mechanism for the formation of NO by fixation of atmospheric $N_2$ allows correction of equilibrium NO values. The result permits rough comparison with actual engine emissions measurements.

The overall reaction for the thermal NO mechanism is:

$$1/2\ N_2 + 1/2\ O_2 ===> NO\ \ + 90.4\ kJ/mol$$
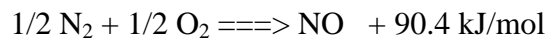
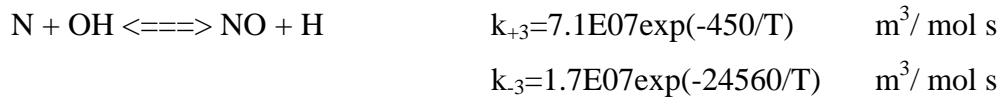This overall reaction is highly endothermic, hence NO is produced only at high temperatures. The reaction actually occurs in two distinct steps:

| | | |
|---|---|---|
| $N_2 + O <===> NO + N$ | $k_{+1}=1.8E08exp(-38,370/T)$ | $m^3/$ mol s |
| | $k_{-1}=3.8E07exp(-425/T)$ | $m^3/$ mol s |
| $N + O_2 <===> NO + O$ | $k_{+2}=1.8E04\ T\ exp(-4680/T)$ | $m^3/$ mol s |
| | $k_{-2}=3.8E03Texp(-20,820/T)$ | $m^3/$ mol s |

The major sink for the N atom is the OH radical:

$$N + OH <===> NO + H \qquad k_{+3}=7.1E07exp(-450/T) \qquad m^3/ \, mol \, s$$
$$k_{-3}=1.7E07exp(-24560/T) \qquad m^3/ \, mol \, s$$

The high activation energy for the first reaction (a result of breaking the strong triple bond of $N_2$) makes this the rate-limiting step. Because of the high activation energy, the rate of this reaction is slower than the oxidation of the fuel and is very temperature sensitive.

Because NO production is slower than fuel oxidation, it forms behind the flame front where the highest temperature and extra residence time exist (because the gas wants to expand but cannot, and because heat has not yet had time to be conducted away).

Hence, to gain a first approximation of NO reaction kinetics without solving the entire gas-phase ethanol combustion mechanism, assume that (O), (H), (OH), and (N) are at steady-state equilibrium values since NO formation occurs after the combustion reactions. Following the arguments presented by Lavoie, et al. [1970], the ratio of the actual NO concentration to the NO concentration at equilibrium can be estimated:

$$\alpha \equiv \frac{[NO]}{[NO]_e} .$$

The characteristic time *required* for NO formation can be approximated as

$$\tau_{NO} = \frac{[NO]_e}{4R_1} ,$$

where $R_1$ is the rate of the first reaction in the Zeldovich mechanism at equilibrium. $\tau_{NO}$ corresponds to the time required if the reaction had continued at its initial rate and was not slowed by reverse reactions.

**Ethanol-Water Products at Equilibrium and**
**Zeldovich Thermal NO Formation**
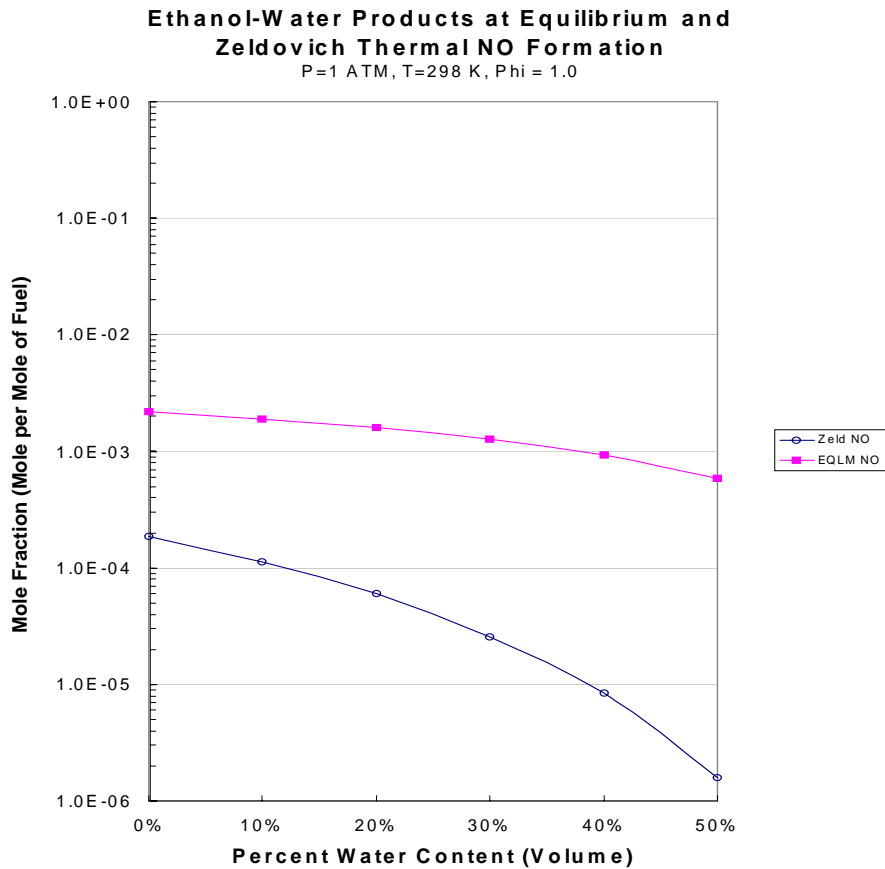P=1 ATM, T=298 K, Phi = 1.0



**Figure 2.3 Mole fraction of NO (per mole of ethanol) vs. fuel water content at equilibrium and at 0.015 seconds.**

The time *available* for NO formation was approximated as 0.015 seconds, the in-cylinder residence time for a 17:1 compression ratio engine operating at 2000 rpm.

The calculation of NO formation using the Zeldovich mechanism falls below the thermodynamic equilibrium results by an order of magnitude at 0 percent water by volume (Fig. 2.3). As the percent of water increases, NO production continues to drop significantly lower than the equilibrium prediction.
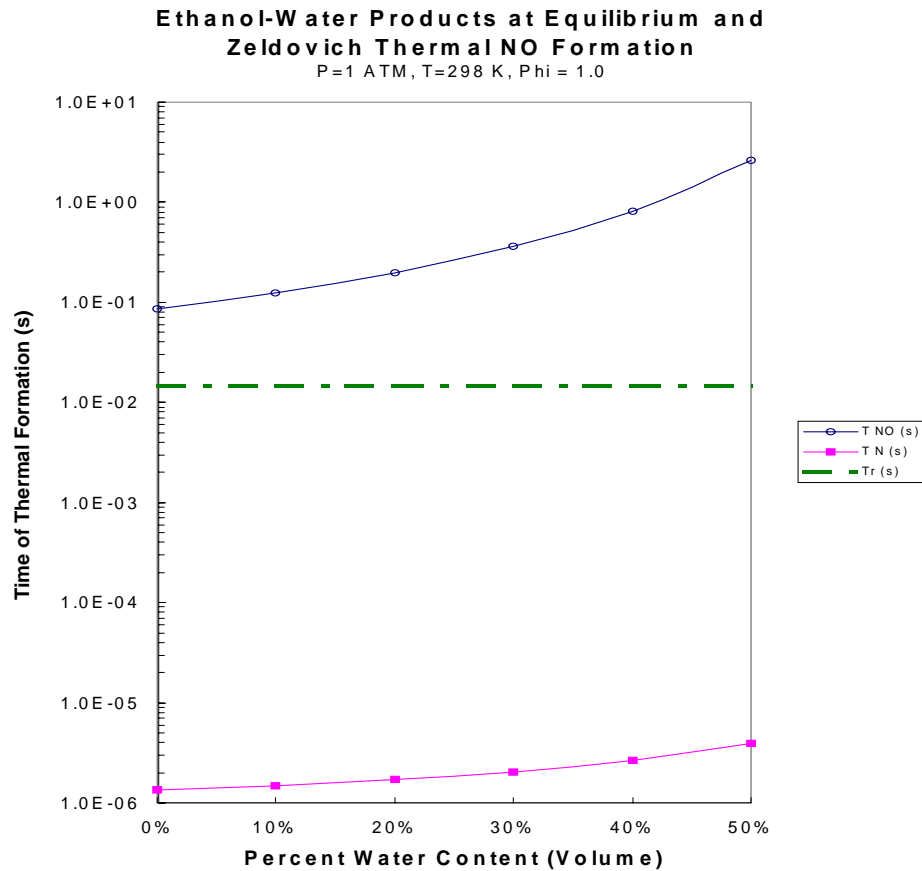
**Figure 2.4 Characteristic time required for NO formation (top curve) and N equilibrium (bottom time) compared with the characteristic in-cylinder residence time as a function of fuel water content.**

At 30 percent water content, Fig. 2.3 indicates that the *estimated* NO production using the Zeldovich mechanism is an order-of-magnitude lower than that for neat ethanol.

At ~30 percent water content, the *measured* NO (as NOx) in the exhaust of a 17:1 compression ignition engine varied from 10 to 25 ppm [Morton, 2000], an order-of-magnitude lower than expected for CI engines operating with "dry" fuel and one-to-two orders-of-magnitude lower than raw exhaust from SI engines operating with conventional fuel. Consequently, the impact of water on NO formation can be roughly explained by the sensitivity of the thermal NO mechanism to decreasing combustion temperature with increasing water-fuel content.

The assumption that there is sufficient time for the radicals to reach steady state concentrations is tested by calculating the characteristic time required:

$$\tau_N = \frac{[N]_e}{R_2 + R_3},$$

where $R_2$ and $R_3$ are the rates of the second and third reactions in the Zeldovich mechanism at equilibrium. Comparison of the two time scales $\tau_{NO}$ and $\tau_N$ in Fig. 2.4 with the characteristic in-cylinder residence time indicates that $\tau_N$ is several orders-of-magnitude shorter than $\tau_{NO}$ and the in-cylinder residence time.

## III. Combustion Kinetics

An exhaustive literature search and a visit to Lawrence Livermore National Laboratory resulted in a database that contains the complete detailed chemical kinetic mechanism for gas-phase ethanol combustion; a FORTRAN program developed at LLNL that evaluates the detailed hydrodynamics, chemical kinetics, and transport for one-dimensional systems; and good headway towards understanding the gas phase reactions as well as the heterogeneous mechanism for ethanol decomposition on platinum in the presence of water.

In order to understand the *gas phase* combustion process of ethanol, first we must examine the structure of ethanol itself. Ethanol is a slightly polar molecule with a bond angle of about 105 degrees between the central carbon atom and the OH radical (Fig. 3.1). This bond angle is similar in size to the water molecule, which is also slightly polar in nature. Because of this similarity, water and ethanol are miscible in all proportions. In concentrations greater than 95 percent, ethanol will extract water out of the air when placed in an open vessel.

The bond strengths of ethanol are a hybrid of propane and methanol. The OH radical on the end of ethanol has the same bond strengths as the OH radical in methanol. The carbon-to-carbon bond is similar in strength to the carbon-to-carbon bonds in propane. Reactions in those parts of the ethanol molecule react in the same way as methanol and propane. Insight
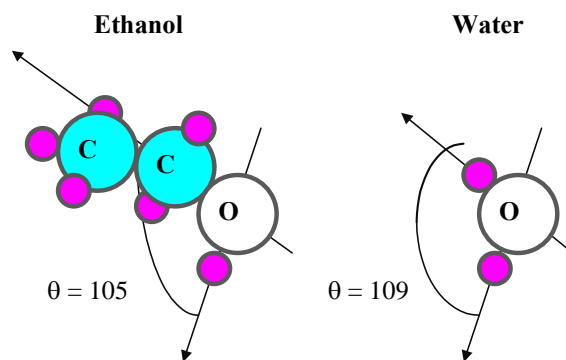
**Figure 3.1 - Bond angles of ethanol and water**

into the reaction properties and mechanisms can be gained by looking at work done on both methanol and propane.

### *Gas-Phase Kinetics*

When ethanol is combusted, it breaks up into three isomers, $CH_3CH_2O$, $CH_3CHOH$, and $C_2H_4OH$, depending on which hydrogen atom is removed. Because of the different bond strengths in the molecule, some reaction mechanisms are more prevalent at one temperature than another. Also, because ethanol can react with several different radicals, there are 15 initial H abstraction reactions that can take place. These reactions are listed in Table 3.1.

**Table 3.1 – Initial Combustion Reactions of Ethanol [Marinov, 1998]**

| No | Reaction | A (cm, s, mol) | b (K) | $E_a$ (kcal/mol) |
|---|---|---|---|---|
| 1 | $C_2H_5OH + OH <= => C_2H_4OH + H_2O$ | 1.74E + 11 | 0.27 | 600.0 |
| 2 | $C_2H_5OH + OH <= => CH_3CHOH + H_2O$ | 4.64E + 11 | 0.15 | 0.0 |
| 3 | $C_2H_5OH + OH <= => CH_3CH_2O + H_2O$ | 7.56E + 11 | 0.30 | 1634.0 |
| 4 | $C_2H_5OH + H <= => C_2H_4OH + H_2$ | 1.23E + 07 | 1.80 | 5098.0 |
| 5 | $C_2H_5OH + H <= => CH_3CHOH + H_2$ | 2.58E + 07 | 1.65 | 2827.0 |
| 6 | $C_2H_5OH + H <= => CH_3CH_2O + H_2$ | 1.50E + 07 | 1.60 | 3038.0 |
| 7 | $C_2H_5OH + O <= => C_2H_4OH + OH$ | 9.41E + 07 | 1.70 | 5459.0 |
| 8 | $C_2H_5OH + O <= => CH_3CHOH + OH$ | 1.88E + 07 | 1.85 | 1824.0 |
| 9 | $C_2H_5OH + O <= => CH_3CH_2O + OH$ | 1.58E + 07 | 2.00 | 4448.0 |
| 10 | $C_2H_5OH + CH_3 <= => C_2H_4OH + CH_4$ | 2.19E + 02 | 3.18 | 9622.0 |
| 11 | $C_2H_5OH + CH_3 <= => CH_3CHOH + CH_4$ | 7.28E + 02 | 2.99 | 7948.0 |
| 12 | $C_2H_5OH + CH_3 <= => CH_3CH_2O + CH_4$ | 1.45E + 02 | 2.99 | 7649.0 |
| 13 | $C_2H_5OH + HO_2 <= => C_2H_4OH + H_2O_2$ | 1.23E + 04 | 2.55 | 15750.0 |
| 14 | $C_2H_5OH + HO_2 <= => CH_3CHOH + H_2O_2$ | 8.20E + 03 | 2.55 | 10750.0 |
| 15 | $C_2H_5OH + HO_2 <= => CH_3CH_2O + H_2O_2$ | 2.50E + 12 | 0.00 | 24000.0 |

There are also four decomposition reactions that can take place. Because ethanol is a multiple atom molecule (Fig. 3.2 top), there are internal forces acting on it. All bonds have vibrational and rotational frequencies associated with it. When an outside molecule that is in synchrony with the vibrational harmonics of an ethanol molecule bumps into it, ethanol can decompose, losing an OH radical (Fig. 3.2 C). When coupled with the rotational frequency, and based on ethanol's geometry, two H radicals in ethanol can drop their bonds with the carbon and oxygen and bond together (Fig. 3.2 B). Water can form from ethanol decomposition (Fig. 3.2 C). The C-C bond can also break—the only initial ethanol reaction where this occurs (Fig. 3.2 D). These situations add four more reactions to the ethanol combustion mechanism (Table 3.2).

**Table 3.2 - Decomposition Reactions of Ethanol [Marinov, 1998]**

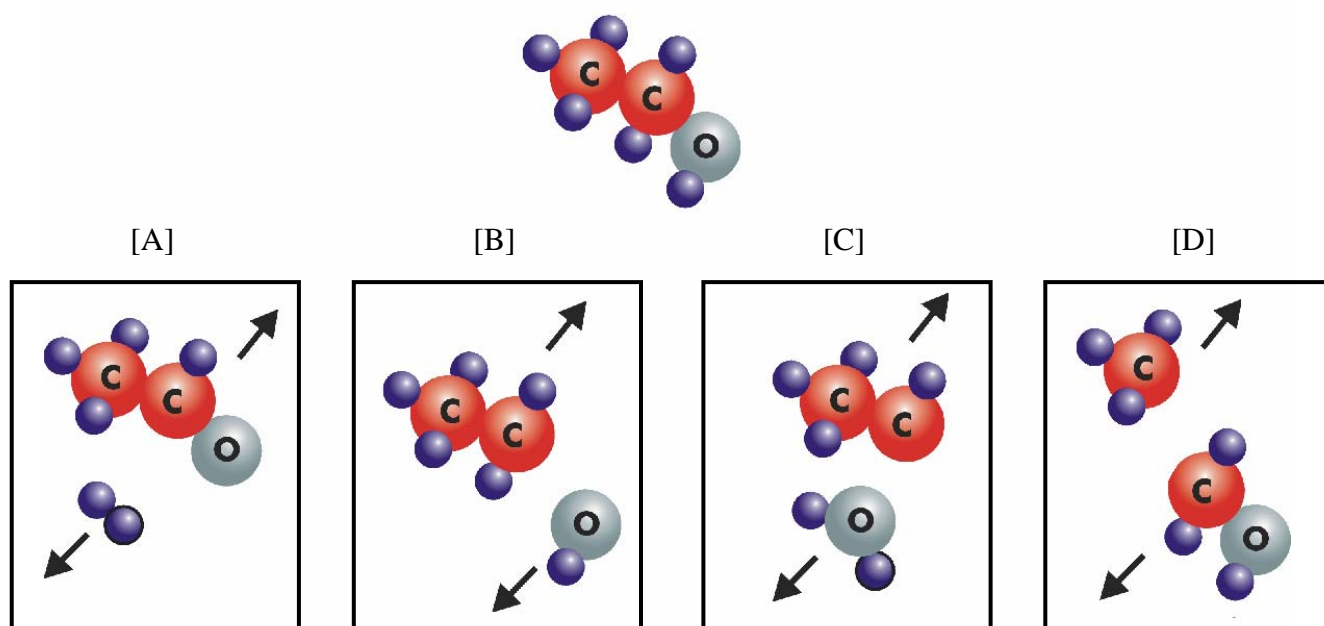| No | Reaction | A (cm, s, mol) | b (K) | $E_a$ (kcal/mol) |
|----|----------|----------------|-------|------------------|
| 16 | $C_2H_5OH + (M) <= => CH_2OH + CH_3 + (M)$ | 5.94E + 23 | -1.68 | 91163.0 |
| 17 | $C_2H_5OH + (M) <= => C_2H_5 + OH + (M)$ | 1.25E + 23 | -1.54 | 96005.0 |
| 18 | $C_2H_5OH + (M) <= => C_2H_4 + H_2O + (M)$ | 2.79E + 13 | 0.09 | 66136.0 |
| 19 | $C_2H_5OH + (M) <= => CH_3HCO + H_2 + (M)$ | 7.24E + 11 | 0.095 | 91007.0 |



[A]     [B]     [C]     [D]

**Figure 3.2 Ethanol decomposition reactions. Top: Ethanol molecule before collision decomposition; A: Formation of $H_2$; B: Formation of OH radical; C: Formation of $H_2O$ molecule; D: C-C bond scission. [Marinov, 1998]**

The main reaction pathways found for stoichiometric homogeneous ethanol combustion in air are sketched in Fig. 3.3 [Egolfopoulos, et al. 1992; Norton and Dryer, 1992]. The initial H abstraction reactions in Table 3.1 dominate.

The most prevelant isomer formed is $CH_3CHOH$, which reacts with oxygen to form acetaldehyde. Ethene is produced from $C_2H_4OH$. The least populous isomer is $CH_3CH_2O$, which forms formaldehyde. Each of the stable intermediaries are potential pollutants, with
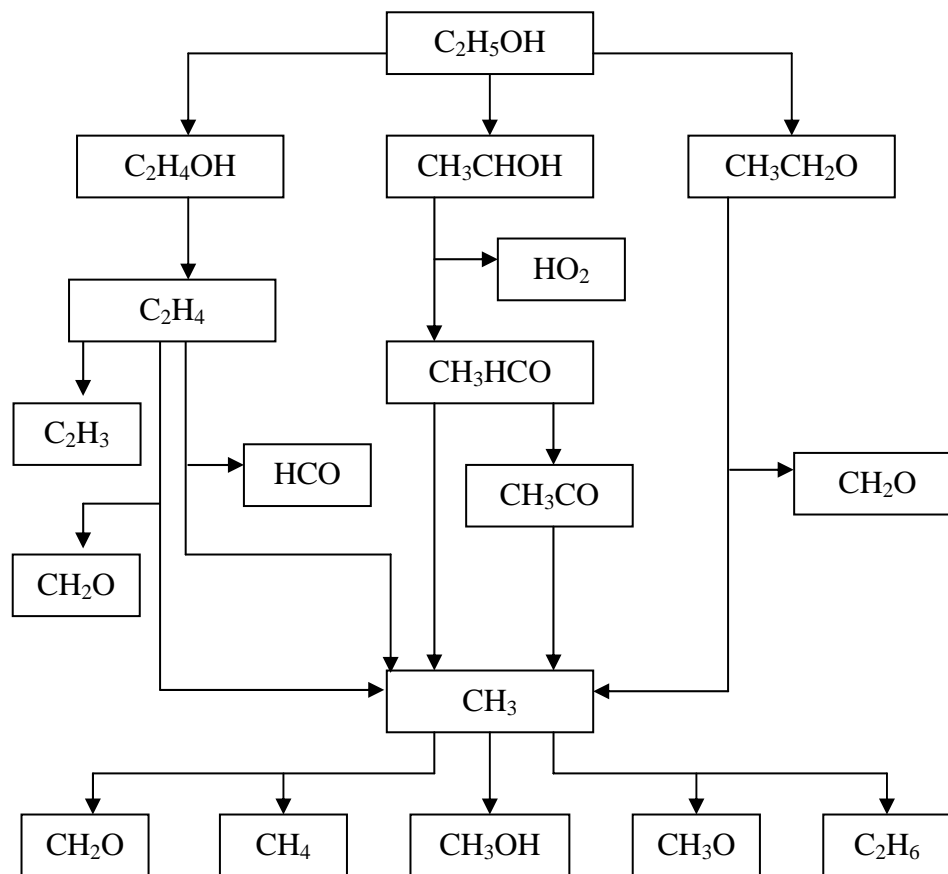
**Figure 3.3   Major pathways for stoichiometric homogeneous combustion of ethanol [Egolfopoulos, et al., 1992; Norton and Dryer, 1992].**

acetaldehyde of particular concern since nearly half of the ethanol can decompose to $CH_3CHOH$ [Norton and Dryer, 1992].

Hydrocarbon emissions from internal combustion engines can occur from quenching in crevice volumes, surface deposits, cold combustion chamber walls, and incomplete fuel air mixing. Acetaldehyde should be present in the exhaust gases because of the quenching near the cylinder walls. Complete combustion would permit acetaldehyde and ethene to eventually decompose to the methyl radical which is the major reaction product from each of the isomers.

The sensitivity analysis performed by Egolfopolous, et al. [1992] found that the reaction

$$C_2H_5OH + OH <= => C_2H_4OH + H_2O$$
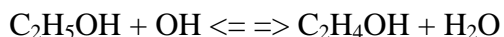
(the first reaction in Table 3.1) was the only reaction uniquely important in ethanol combustion. Other important reactions—the chain branching reaction and CO oxidation:

$$H + O_2 <= => OH + O$$

$$CO + OH <= => CO_2 + H,$$
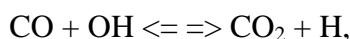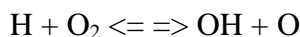
are found to be important in hydrocarbon combustion in general.

Because of the importance of the reaction $C2H5OH + OH <= => C2H4OH + H2O$ in ethanol combustion, increased production of OH radicals through modest water dissociation or catalyst production would favor flame propagation.

### *Surface reactions of ethanol and water—Pt-ethanol major reaction pathways*

Catalysts increase the rate of a reaction without being consumed by the reaction. This is effectively achieved by lowering the activation energy. Although a catalyst permits chemical equilibrium to be reached faster, it cannot change where equilibrium occurs. Hence, the relative energies of products and reactants remain the same. Only spontaneous reactions can be catalyzed.

In general, the metal catalysts work on oxygenated gases by adsorbing the gases on their surface. A weak bond forms between the oxygen atom and the metal. The formation of this bond weakens adjacent bonds, thus requiring less energy for the molecule to break via surface reactions [Cho and Law, 1986]. Product desorption follows the surface reactions. Because the surface of the catalyst is recovered after a sequence of reactions, the surface can catalyze reactions repeatedly. Hence, a small amount of catalyst produces a large effect.

A relationship also exists between the thermodynamics of a reaction and the activation energy. As the reaction becomes more exothermic, the activation energy decreases. If everything else is equal on the surface, an elementary reaction with low intrinsic activation

energy will precipitate a reaction pathway that dominates over a pathway precipitated by an elementary reaction with a high intrinsic barrier [Mosel and Ti, 1997].

Ethanol is composed of two carbon atoms, one oxygen atom and six hydrogen atoms. The bond strengths between the atoms can help determine what reactions will take precedence on the platinum surface. The bonds between the carbon and hydrogen are approximately 98 kcal/mol while the bonds between oxygen and hydrogen are approximately 104 kcal/mol. It is interesting to note that the bond between the two carbon atoms is only approximately 83 kcal/mol, which is also about the same as the carbon-oxygen bond at 84 kcal/mol. Looking at just the bond strengths, it would be easy to assume that the carbon-carbon and carbon-oxygen bonds would be the first to break. However, the hydrogen atoms are stripped off first because of the proximity effect of the platinum surface. The ethanol becomes chemisorbed to the
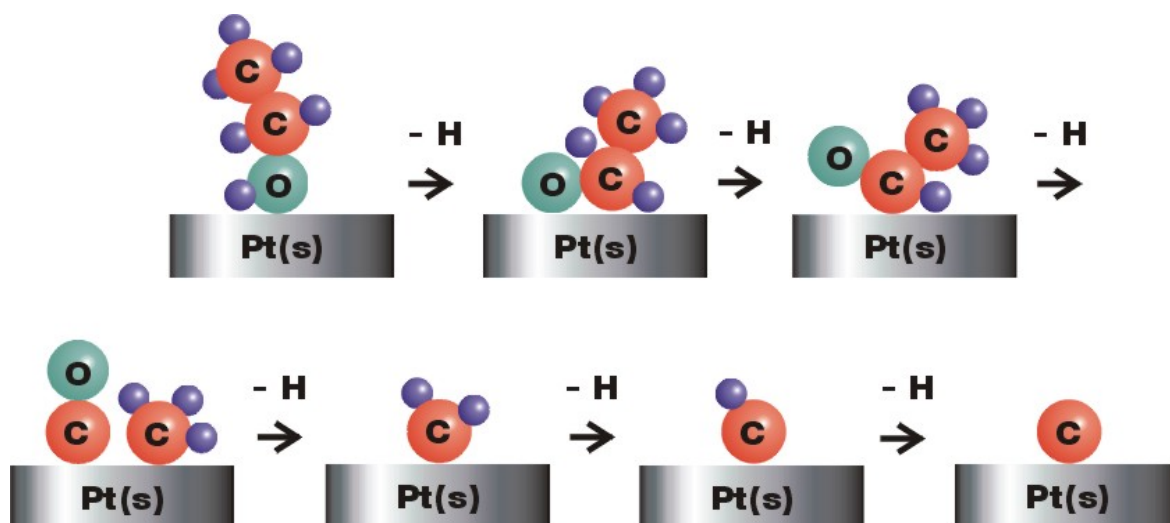


Figure 3.4 Decomposition of ethanol on Pt at high temperature [Masel, 1996]

platinum surface, which can significantly reduce adjacent bond energies [Masel, 1996; Cho and Law, 1986].

Because ethanol is polar, the molecule aligns itself to the surface with the oxygen-hydrogen bond nearest to the surface. When the molecule reaches a proximity limit, an oxygen-surface bond forms (Fig. 3.4, step 1), weakening the oxygen-hydrogen bond. The hydrogen attached

to the oxygen is the first atom to be stripped away from the molecule even though the bond strength is higher than the other bonds in the molecule.

Next, based on molecular geometry, the newly formed ethoxy radical folds over and again a hydrogen radical is stripped away due to bond weakening from the molecule-surface proximity (Fig. 3.4, step 2). When the second hydrogen is stripped away, the carbon re-associates with the oxygen atom, forming a double bond. This keeps the core of the ethanol molecule together while the hydrogen is being stripped away.

The new double bond is harder to break than the single carbon-hydrogen bonds. Not until all of the central carbon's hydrogen atoms are stripped away can the central carbon atom get close enough to the surface to form a proximity bond (Fig. 3.4, step 3). The ethanol is now reduced to $CH_3CO$ - and the mechanism changes.

Now the mechanism favors a carbon-carbon scission. The carbons split and a triple bond is formed with the oxygen (Fig. 3.4, step 4). Carbon monoxide is released from the platinum surface (with a desorption activation energy of only 30 kcal/mol [Goralski, et al., 1999; Deutschmann, et al., 1994]) and the surface is left with a methyl radical [Masel and Lee 1996].

No data—sticking coefficients, pre-exponential coefficients, or activation energies—could be found for the adsorption and surface reactions of ethanol. Once ethanol is reduced to CO and the methyl radical, data can be found for surface and desorption reactions. For example, the methyl radical can continue to decompose through surface interactions (Fig. 3.4, steps 5, 6, and 7). The pre-exponential constant and activation energy for an Arrhenius-type behavior have been reported [Deutschmann, et al., 1994].

Remaining C(s) can react with O(s) (from the decomposition of adsorbed $O_2$) to form CO, which desorbs. Surfaces reactions of H(s) and O(s) form OH(s), which can desorb with an activation energy of 46 kcal/mol following an Arrhenius-type form.

Desorption of OH was the only example found of a radical escaping the Pt surface. At high temperature, it may be possible for other radicals to desorb. Stable desorption products include $O_2$, $H_2O$, $CO$, and $CO_2$.

### *Surface reactions of ethanol and water—Pt-water reactions*

Water is also a slightly polar molecule. It adheres to the platinum surface with a sticking coefficient of 0.75 (the sticking coefficient is the probability that a molecule remains on the surface after a collision). Thus water can take available reaction sites away from ethanol. However, once water adsorbs, two surface reactions that produce OH are possible (Table 3.3). Platinum will also create water from H and OH radicals, thus removing them from the reaction process.

The water vapor in the fuel mixture increases the oxidation of $CO$ to $CO_2$ in the presence of a catalyst. This could be the result of OH radicals produced on the surface of the platinum due to the presence of water at high temperatures [Brunno, et al., 1983] and the subsequent impact on the reaction $CO + OH <= => CO_2 + H$.

**Table 3.3  Water-Pt Reactions [Goralski, et al., 1999; Warnatz, et al., 1999, Deutschmann et al., 1996,1994]. S, A, and $E_a$ are the sticking coefficient, pre-exponential constant, and activation energy.**

| Reaction | S | A (cm, mol, s) | $E_a$ (kcal/mol) |
|---|---|---|---|
| Adsorption | | | |
| $H_2O + Pt(s) <= => H_2O(s)$ | 0.75 | | 0.0 |
| Surface Reactions | | | |
| $H_2O(s) + Pt(s) <= => H(s) + OH(s)$ | | $3.8 \times 10^{21}$ | 17.7 |
| $H_2O(s) + O(s) <= => OH(s) + OH(s)$ | | $1.2 \times 10^{21}$ | 8.2 |
| $OH(s) + Pt(s) <= => O(s) + H(s)$ | | $1.2 \times 10^{22}$ | 19.6 |
| $OH(s) + OH(s) <= => H_2O(s) + O(s)$ | | $3.7 \times 10^{21}$ | 0.0 |
| $H(s) + OH(s) <= => H_2O(s) + Pt(s)$ | | $3.7 \times 10^{21}$ | 4.1 |
| $H(s) + O(s) <= => OH(s) + Pt(s)$ | | $3.7 \times 10^{21}$ | 2.7 |
| Desorption | | | |
| $H_2O(s) <= => H_2O + Pt(s)$ | | $1.0 \times 10^{13}$ | 9.6 |
| $OH(s) <= => OH + Pt(s)$ | | $1.0 \times 10^{13}$ | 46.1 |
| $2H(s) <= => H_2 + 2Pt(s)$ | | $3.7 \times 10^{21}$ | 16.1 |
| $2O(s) <= => O_2 + 2Pt(s)$ | | $3.7 \times 10^{21}$ | 50.9 |

## *Surface reactions of ethanol and water —3.4 Pt surface geometry effect*

The catalyst surface geometry can also play a role in which reaction mechanisms will be the dominant path in the surface chemistry. The atomic planes of a material have been categorized based on the stacking geometry of the atomic structure of the material. Because the platinum molecule and atom are one and the same, platinum is considered to be a FCC (front cubic centered) structure. All atoms in the metal are the same size with the same properties. In the case of platinum, there are several surfaces that can be evaluated depending on how the surface is created and exposed.

The most common is Pt (111) (Fig. 3.5). This represents a surface where all exposed atoms are on the same plane and arranged in a closed packed formation. This arrangement allows attraction sites at any location along the surface.
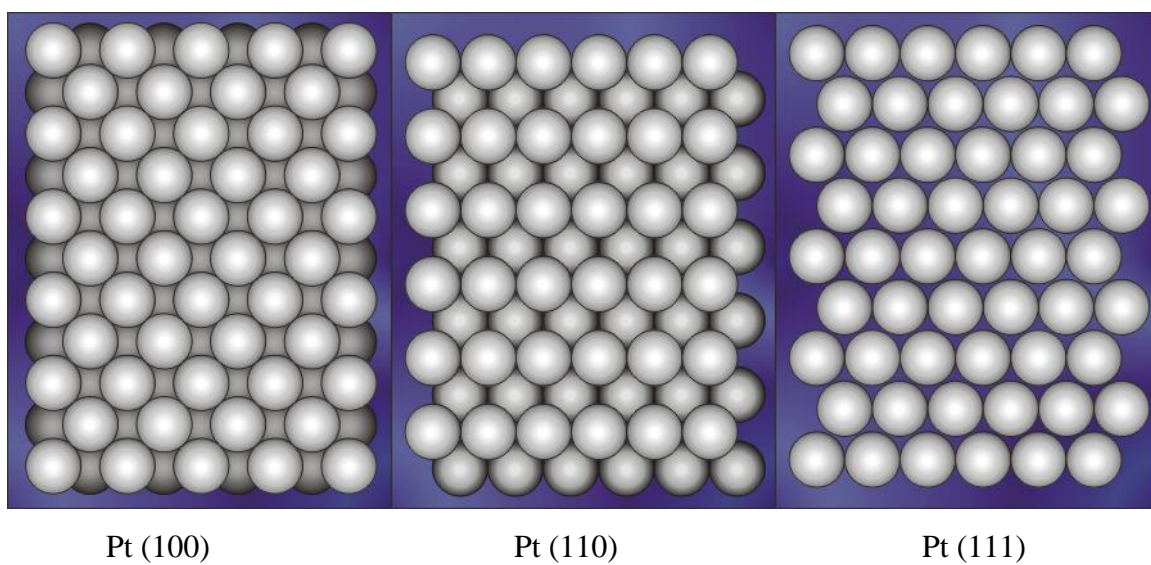
Pt (100)                    Pt (110)                    Pt (111)

**Figure 3.5  Stacking arrangement of platinum [R. Masel, 1996]**

Pt (110) is another main plane of a crystal structure. The atoms are arranged in a two level hexagonal layout (four Pt atoms have an additional Pt atom centered above and another below). This layout forms spaces between the different levels of atoms, which reduces the number of sites that are available for absorption to the surface. It also prevents motion along the surface in certain directions. Also, because of the stretching needed to allow the hydrogen stripping to take place, ethanol breaks down following a *different reaction mechanism* than with other surfaces. In this case the ethanol breaks down into ethene because the ridged surface and the limited motion causes a bond with the second carbon atom (Fig. 3.6). The ethene formed on the surface can continue to decompose on the Pt (Fig. 3.7).
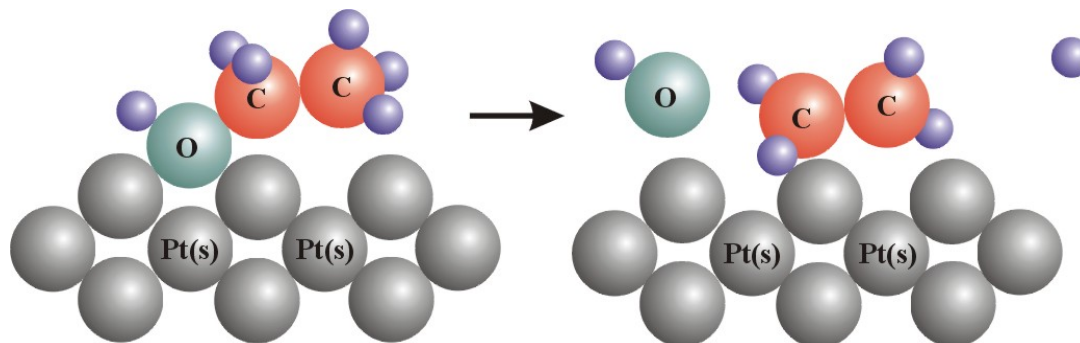


**Figure 3.6 Breakdown of ethanol on Pt(110) [Masel and Lee, 1997]**

The last main surface is Pt (100). The atoms are arranged in a square lattice. This arrangement also allows good mobility along the surface for the reactions to take place [Masel, 1996].
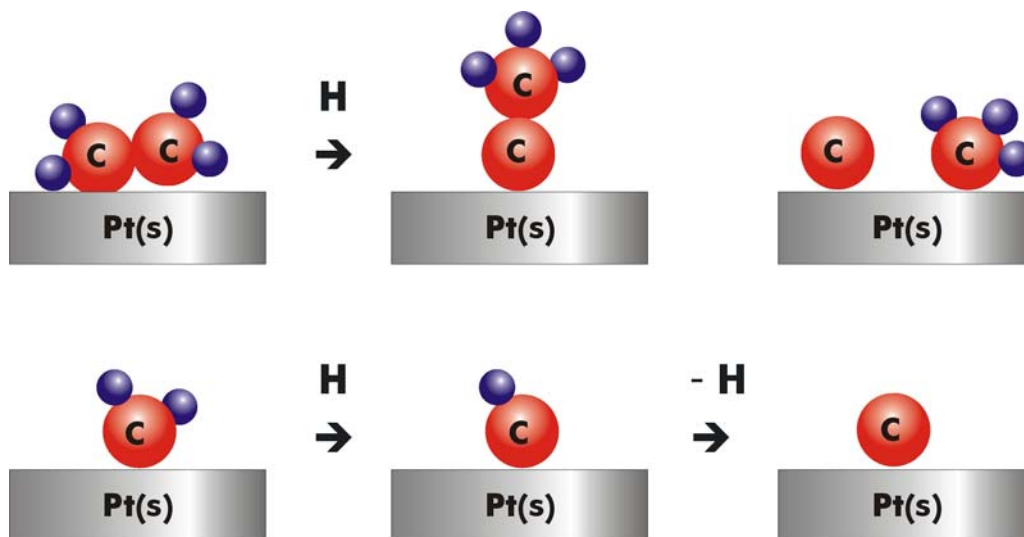


**Figure 3.7 Breakdown of ethene on Pt(110) at high temperature  [Masel and Lee, 1997]**
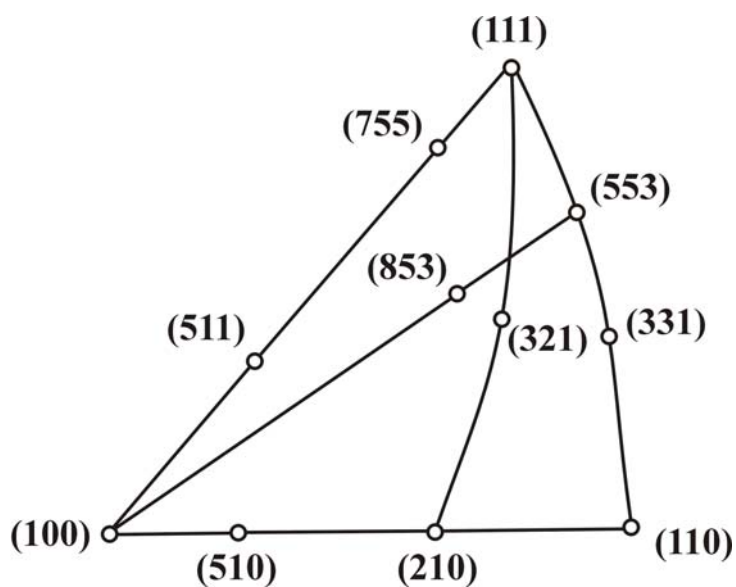


**Figure 3.8 Surface plane geometries [Masel, 1996].**

There are many other surfaces that are formed by cutting a plane in the material somewhere in between the angles needed for a main plane exposure. Figure 3.8 gives a diagram of some of the main geometries used in various studies. All surface geometries can be derived from a combination of the three main geometries discussed above. Ethanol breaks down according to the same pattern under most other geometries except for Pt (110) [Masel and Lee, 1997].

For the practical catalytic igniter, the main sequence discussed first is the dominant method of ethanol decomposition (Table 3.4). Almost every surface will cause ethanol to decompose along this prescribed path, instead of the path characterized by the formation of ethene. With the irregularities in the platinum surface on the igniter, in most cases the bond length does not have to be stretched in order for the hydrogen to be stripped off the molecule. Surface irregularities may make the reaction take place more easily. Consequently, using an amorphous platinum wire or paste will not significantly change the reaction mechanisms.

**Table 3.4 Dominant reduction mechanism of ethanol on Pt [Masel, 1996].**

**Adsorption**

$CH_3CH_2OH + Pt(s) <= => CH_3CH_2OH(s)$

**Surface Reactions**

$CH_3CH_2OH(s) + Pt(s) <= => CH_3CH_2O(s) + H(s)$

$CH_3CH_2O(s) + Pt(s) <= => CH_3CHO(s) + H(s)$

$CH_3CHO(s) + Pt(s) <= => CH_3CO(s) + H(s)$

$CH_3CO(s) + Pt(s) <= => CH_3(s) + CO(s)$

*Temperature effect*

At low catalyst temperatures, the reactions over the surface increase the production of radicals exponentially with a rise in temperature (Fig. 3.9). As the temperature increases beyond this point, catalytic activity is suppressed because the mass diffusion of the reactant to the surface becomes rate limiting. At higher temperatures, the radical production increases

very dramatically and the gas phase combustion works concurrently with the surface reaction [Eguchi and Arai, 1996].
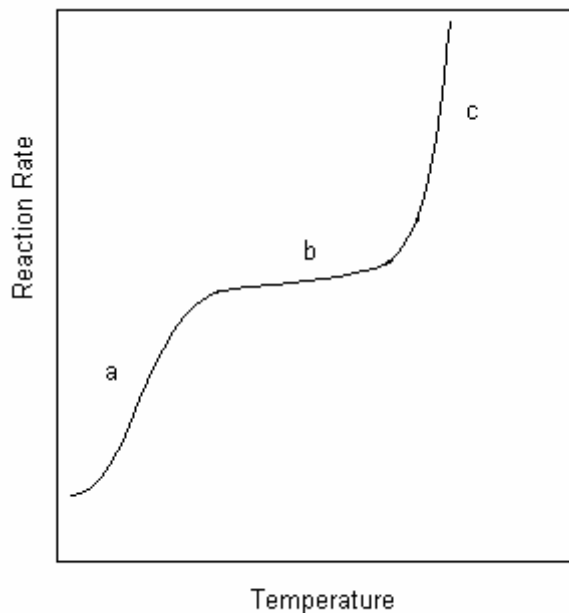


**Figure 3.9 Temperature dependence of catalyst surface reactions: a) low temperature, surface kinetics controlled region; b) mass diffusion controlled region; c) catalyst stabilized thermal combustion [Eguchi and Arai, 1996].**

At low catalyst temperatures, H and OH radicals on the surface can form water, which blocks sites from reaction with other species. The sites would not be freed until water desorbs. This explains why the catalytic injector has to be heated until operating temperatures are achieved. The catalyst surface on the igniter core has to reach the high temperature region where catalytically stabilized thermal combustion can be maintained through heat generated in the combustion process.

The mechanisms illustrated in Fig. 3.4, 3.6 and 3.7 also change with temperature. At low temperature, the methyl radical reacts with H to form methane, which desorbs. Higher catalyst temperature is required for the complete decomposition of the methyl radical [Masel, 1996].

## Hydrodynamics, Combustion, and Transport (HCT) Code

The HCT code originated at Lawrence Livermore National Laboratory in the 1970s as an aid to develop detailed chemical kinetics mechanisms in combustion [Lund, 1995]. Written in FORTRAN on UNIX workstations, the program was ported to the Windows environment.

HCT is a finite-difference code that calculates one-dimensional time-dependent problems involving gas hydrodynamics, transport, and detailed chemical kinetics. It can calculate ignition occurrence, unsteady flame velocity, steady state flame propagation, and species mole fractions. The code solves the coupled equations for the conservation of mass, momentum, energy, and the conservation of each chemical species (Table 3.5). The inherently stiff set of equations is solved implicitly using LU decomposition.

**Table 3.5 Model Equations**

| | |
|---|---|
| $\dfrac{\partial \rho}{\partial t} + \dfrac{\partial \rho u}{\partial x} = 0$ | Conservation of mass |
| $\dfrac{\partial \rho u}{\partial t} + \dfrac{\partial \rho u^2}{\partial x} = -\dfrac{\partial (P+Q)}{\partial x}$ | Conservation of momentum |
| $\dfrac{\partial \rho \zeta}{\partial t} + \dfrac{\partial \rho u h_s}{\partial x} = \dfrac{\partial}{\partial x}\left(\rho C_P a \dfrac{\partial T}{\partial x}\right) + \dfrac{\partial}{\partial x}\left(\rho \sum h_i D_i \dfrac{\partial y_i}{\partial x}\right) + \rho q$ | Conservation of energy |
| $\dfrac{\partial \rho y_i}{\partial t} + \dfrac{\partial \rho u y_i}{\partial x} = \dfrac{\partial}{\partial x}\left(\rho D_i \dfrac{\partial y_i}{\partial x}\right) + (\rho y_i)_{kin}$ | Conservation of species $i$ |

In Table 3.5, the following nomenclature is used:

$C_p$ – specific heat (kJ/kg-K)      $u$ – velocity (m/s)

$D$ – diffusion coefficient (kg/m-s)      $y$ – mass fraction (kg/kg)

$h$ – enthalpy (kJ/kg)      $\alpha$ – thermal diffusivity (m/s$^2$)

$P$ – pressure (N/m$^2$)      $\zeta$ – internal energy (kJ/kg)

$Q$ – work (kJ/m$^3$)      $\rho$ – density (kg/m$^3$)

$q$ – rate of heat generation by
    chemical reaction (kW/kg)

---

Our goals for working with the HCT code are listed as follows:

- o Complete porting all the programs to PC Windows.
- o Start with gas-phase combustion to learn how the code works and also to see the impact of water on gas-phase ethanol combustion.
- o Continue search for initial ethanol-Pt decomposition reaction data.
- o Develop a 1-D model for catalyst surface reactions.
- o Incorporate the surface reaction model as a new subroutine in HCT.
- o Model the coupled homogeneous-heterogeneous catalytically assisted ignition of ethanol-water fuel.

Because the source code for HCT will be changed as a result of this project, the program's logic and structure must be understood to a high degree of detail. Problems solved by HCT are broken into zones where temperature, pressure, and species concentration are held constant. The zones can be of variable length for better resolution in regions of high temperature gradients. Essentially, HCT functions as a generic solver with a pre-processing program (MCKDAT) and post-processing programs (TRDMP and HCTPLT) (Fig. 3.10)

MCKDAT updates a database of species thermodynamic data and chemical reaction kinetic data and creates the binary input file cdat for HCT. The thermodynamic data includes polynomial data for the specific heat in the NASA database format, from which enthalpy and the Gibbs function can be calculated. The chemical reaction kinetic data includes the pre-exponential constant ($A$) the temperature sensitivity ($b$) and the activation energy ($E_a$) for each of the hundreds of elementary reactions (372) in the gas-phase ethanol combustion mechanism.
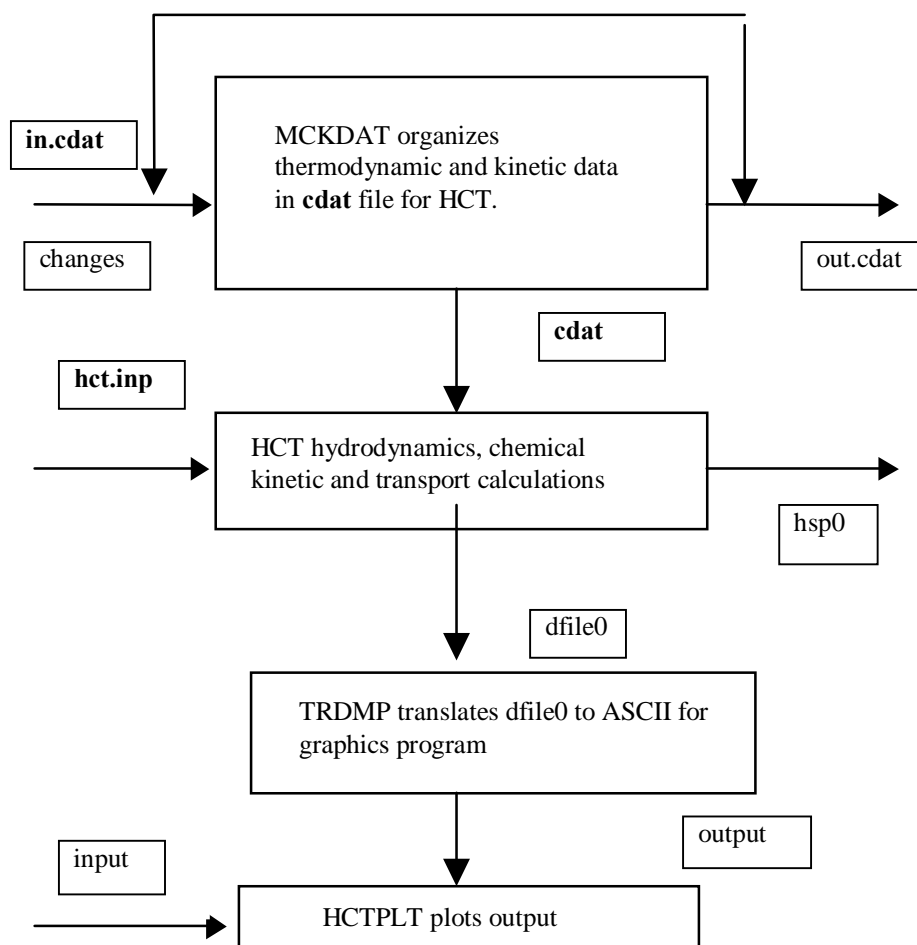
**Figure 3.10 Logic flow and file interaction for the
MCKDAT, HCT, TRDMP, and HCTPLT programs.**

The chemistry database is contained in the ASCII file in.cdat. MCKDAT updates
in.cdat with changes and stores it as out.cdat, and creates the binary file cdat for HCT.
The updated database out.cdat is then renamed as in.cdat for use in the next problem.

The other input file needed by HCT, hct.inp, describes the physical problem and how the
problem is to be executed. This input file is created by editing a file from a prior problem.
Here, pointers are used to select the species and reactions needed from cdat for the chemical
kinetic mechanism of the problem. Data for a specific reaction can be corrected by entering
data that will override the data in cdat. Comments can be liberally used to document the
problem. Information about zones is added here.

After HCT completes the combustion calculations, the results are printed in a file hsp0. The file dfile0 is also created to store data for re-starting the calculation, and for input to TRDMP, which translates dfile0 into ASCII for graphics applications. HCTPLT reads the TRDMP output and graphs results per the users specifications in the HCTPLT input file: mole fractions, velocity, temperature and zone width vs. distance.

*One-Dimensional Catalytic Ignition Model*

A simplified graphic of the one-dimensional catalytic combustion model is presented in Fig. 3.10. Unreacted fuel and air are convected to the catalyst surface where ethanol and water molecules are adsorbed onto the Pt surface and decompose following mechanisms discussed above. Reactions between the decomposition products also occur on the surface. Desorbed radicals and stable products, and heat released during surface reactions, diffuse into the unreacted layer of fuel above the surface where gas-phase ignition occurs.



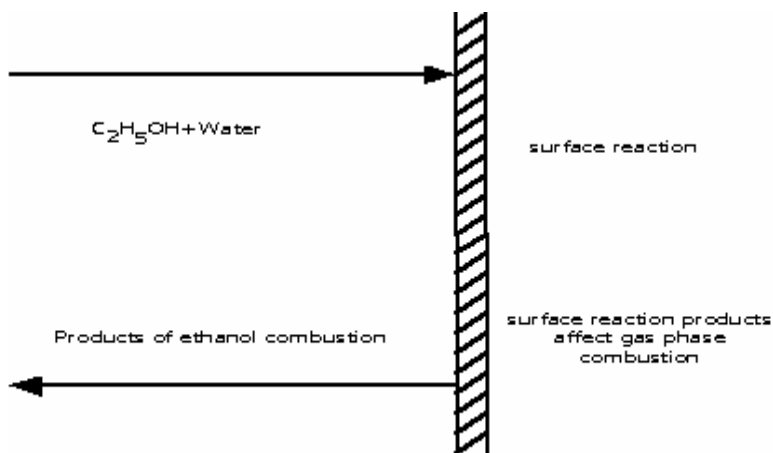**Figure 3.11 One-dimensional model for heterogeneous combustion.**

*Summary*

- The design and construction of the reactor is well underway. At the invitation of colleagues, we traveled to Drexel University and Penn State to visit pressurized flow reactors for fundamental combustion studies. This trip permitted us to obtain in-depth knowledge of the reactors that is not archived in the literature. The

vaporization section has been built. A prototype mixing nozzle has been machined and will be tested as a senior laboratory project.

- The thermodynamic equilibrium calculations are finished for ethanol-water volume fractions ranging from 0 to 0.5; equivalence ratios ranging between 0.4 and 1.6 (fuel lean to fuel rich) and pressures ranging from 1 to 16 atmospheres. The calculations verify the influence of the water-gas shift reaction on the increased oxidation of carbon monoxide with increased fuel water content. By including the chemical kinetics of the extended Zeldovich reaction for fixation of atmospheric nitrogen, we explained trends observed in the measurements of NO emissions.

- Good progress has been made in the understanding of the gas phase and surface reactions of ethanol. A detailed mechanism exists for gas-phase combustion of ethanol, including all the data needed for thermodynamic and chemical kinetic calculations. The Pt-catalyzed decomposition mechanism of ethanol is understood physically, but data is lacking for the initial reactions. The MCKDAT and HCT programs have been ported to PC Windows.

## REFERENCES

Cherry, M. A., and C. L. Elmore, "Timing chamber ignition method and apparatus," *US Patent* 4,977,873, December 18, 1990.

Cherry, M. A., "Catalytic-compression timed ignition," *US Patent* 5,109,817, May 5, 1992.

Cherry, M. A., R. J. Morrisset, and N. J. Beck, "Extending lean limit with mass-timed compression ignition using a catalytic plasma torch," *Society of Automotive Engineers,* Paper *921556,* 1992.

Cho, P. and C. K. Law, "Catalytic ignition of fuel/oxygen/nitrogen mixtures over platinum," *Combustion and Flame,* Vol. 66, pp.159-170, 1986.

Dagaut, P., M. Cathonnet, J. P. Rouan, R. Foulatier, A. Quilgars, J. C. Boettner, F. Gaillard, and H. James, "A jet-stirred reactor for kinetic studies of homogeneous gas-phase reactions at pressures up to ten atmospheres (~1 MPa)," *Journal of Physics E: Scientific*, 1986, Vol. 19.

Deutschmann, O., R. Schmidt, F. Behrendt, and J. Warnatz, "Numerical modeling of catalytic ignition," *Twenty-Sixth International Symposium on Combustion*, The Combustion Institute, pp. 1747-1754, 1996.

Deutschmann, O., F. Behrendt, and J. Warnatz, "Modeling and simulation of heterogeneous oxidation of methane on a platinum foil," *Catalysis Today*, Vol. 21, p. 461, 1994.

Dryer, F.L., "High temperature oxidation of carbon monoxide and methane in a turbulent flow reactor," *AMS Report* T-1034, 1972

Egolfopolous, F. N., D. X. Du, C. K. and Law, "A study on ethanol oxidation kinetics in laminar premixed flames, flow reactors, and shock tubes," *Twenty-Fourth International Symposium on Combustion*, The Combustion Institute, pp. 833-841, 1992.

Eguchi, K. and H. Arai, "Recent advances in high temperature catalytic combustion," *Catalysis Today*, Vol. 29, pp. 379-386, 1996.

Goralski Jr., C. T., and L. D. Schmidt, "Modeling heterogeneous and homogeneous reactions in the high-temperature catalytic combustion of methane," *Chemical Engineering Science*, Vol. 54, pp. 5791–5807, 1999.

Hoffman, J. S., W. Lee, T. A. Litzinger, D. A. Santavicca, and W. J. Pitz, "Oxidation of propane at elevated pressures: experiments and modeling," *Combustion Science and Technology*, Vol. 77, pg. 95-125, 1991.

Kaiser, E.W., C. K. Westbrook, and W. J. Pitz, "Acetaldehyde oxidation in the negative Temperature coefficient regime: experimental and modeling results," *International Journal of Chemical Kinetics*, Vol. 18, pp. 655-688, 1986.

Karim, H., L. D. Pfefferle, P. Markatou, and M. Smooke, "Modeling heterogeneous/ homogeneous reactions and transport coupling of catalytic combustion of methyl chloride over a Mn-based catalyst," *Twenty-Fifth International Symposium on Combustion*, pg. 299-306, 1994.

Koert, D. N.. *Effects of Pressure on Hydrocarbon Oxidation Chemistry*. Doctor of Philosophy Thesis, Drexel University, 1990.

Lavoie, G. A., J. B. Heywood, and J. C. Keck, "Experimental and theoretical study of nitric oxide formation in internal combustion engines," *Combustion Science and Technology*, Vol. 3, pp. 313-326, 1970.

Lund, C. M., "HCT: A general computer program for calculating time-dependent phenomena involving one-dimensional hydrodynamics, transport, and detailed chemical kinetics," revised by L. Chase, *Lawrence Livermore National Laboratory, UCRL-52504*, 1995.

Mao, F., and R. B. Barat, "Experimental and modeling studies of staged combustion using a reactor engineering approach," *Chemical Engineering Communication*, Vol. 145, pg. 1-21, 1996.

Marinov, N. M., "A detailed chemical kinetic model for high temperature ethanol oxidation," *U.S. Department of Energy/Lawrence Livermore National Lab,* Contract W-7405-ENG-48, 1998.

Marr, J. A., D. M. Allison, L. M. Giovane, L. A. Yerkey, P. Monchamp, J. P. Longwell, and J. B. Howard, "The effect of chlorine on PAH, soot, and tar yields form a jet stirred/plug flow reactor system," *Combustion Science and Technology*, Vol. 85, pp. 65-76, 1992.

Masel, R. I. *Principles of Adsorption and Reaction on Solid Surfaces*. New York: John Wiley and Sons, Inc., 1996.

Masel, R. I., and W. T. Lee, "Intrinsic activation barrier as a guide to mechanisms of reactions in the gas phase and on solid surfaces," *Journal of Catalysis*, Vol. 165, pp. 80-90, 1977.

Mitchell, W. L., T. A. Litzinger, and W. Lee, "Effects of in-cylinder catalysts on combustion and emissions of a D.I. diesel engine fueled on neat methanol," *Society of Automotive Engineers,* Paper #920688, 1992.

Morton, Andron. *Homogeneous Charge Combustion of Aqueous Ethanol in a High Compression Catalytic Engine*. Master of Science Thesis, University of Idaho, 2000.

Mosel, R. I., and W. and Ti, "Intrinsic activation barrier as a guide to mechanisms of reactions in the gas phase and on solid surfaces," *Journal of Catalysis*, Vol. 165, pp. 80-90, 1997.

Mueller-Dethlefs, K., and A. F. Schlader, "The effect of steam on flame temperature, burning velocity and carbon formation in hydrocarbon flames," *Combustion and Flame*, Vol. 27, pp. 205-215, 1976.

Norton, T. S., F. L. Dryer, "An experimental and modeling study of ethanol oxidation kinetics in an atmospheric pressure flow reactor," *International Journal of Chemical Kinetics*, Vol. 24, pp. 319 – 343, 1992.

Norton, T. S., and F. L. Dryer, "The flow reactor oxidation of C1-C4 alcohols and MTBE," *Twenty-Third Symposium (International) on Combustion*, The Combustion Institute, pp. 179-185, 1990.

Schwartz, A., L. L. Holbrook, H. Wise, "Catalytic oxidation studies with platinum and palladium," *Journal of Catalysis*, Vol. 21, pg. 199-207, 1971.

Vermeersch, M. L., Held, T. J., Stein, Y., Dryer, F. L., "Auto-ignition chemistry studies of n-butane in a variable pressure flow reactor," *Society of Automotive Engineers,* Paper #912316.

Westbrook, C. K., and F. L. Dryer, "Simplified reaction mechanisms for the oxidation of hydrocarbon fuels in flames," *Combustion Science and Technology*, Vol. 27, pp. 31-43, 1981.

## APPENDIX

**Extramural Funding**

| Source of Support (Granting Agency) | Project Title | Amount of Award | Period Covered by Award |
|---|---|---|---|
| **DoD EPSCoR** | Catalytic Ignition as a Tool for Converting Small Engines to Efficient JP-8 Operation | $384,000 | 4/17/00-4/16/03 |
| **NASA** | Research Cluster | $25,000 | 7/1/99 – 6/30/00 |
| **University of Idaho** | Research Office Seed Grant | $5,999 | 7/1/99 – 6/30/00 |
| **NASA** | Travel Award | $700 | 7/1/00 – 6/30/01 |
| **Micron Technology** | Equipment Grant | $50,000 | July 2000 |
| **NASA** | Graduate Student Fellowship | $6,000 | 7/1/00 – 6/30/01 |
| **GSA** | Graduate Student Travel Award | $550 | November 2001 |

**Publications and Presentations**

| | | |
|---|---|---|
| Society of Automotive Engineers—Small Engine Technology Conference | "Aqueous Ethanol Fueled Catalytic Ignition Engine," SAE Paper 99SETC-5 | September 1999 |
| Army Research Office Contractors Meeting | Catalytic Ignition as a Tool for Converting Small Engines to Efficient JP-8 Operation | June 2000 |
| Drexel University Mechanical Engineering Symposia Series | Catalytic Ignition of Aqueous Ethanol in Conventional SI and CI Engines | November 2000 |
| Joint Meeting of the USA Sections of the Combustion Institute | Theoretical Behavior of Platinum Catalyzed Ethanol-Water Oxidation | March 2001 |